IL NUOVO CIMENTO Vol. 37 C, N. 2 Marzo-Aprile 2014
DOI 10.1393/ncc/i2014-11729-y

Colloquia: LC13

ILC from physics to detector

E. Kato
Tohoku University - Sendai, Japan

ricevuto il 22 Gennaio 2014

Summary. — There is high expectation that measuring precise properties of the Higgs boson will point us to the direction of new physics beyond the standard model. With the discovery of the Higgs boson at the Large Hadron Collider there is a strong demand to conduct an extensive study of the particle, in addition to direct search of new physics. The International Linear Collider is a next generation electron positron collider capable of measuring all major Higgs couplings predicted by the standard model. Currently state-of-the-art detector technologies are being developed to enable high precision measurements.

PACS 13.6.Bc – Electron-positron collisions.
PACS 29.20.Ej – Linear accelerators.
PACS 29.40.-n – Radiation detectors.

1. – The Higgs boson as a probe for physics beyond the Standard Model

Particle physics seeks for a unified understanding of particles and their interactions. The $U(1) \times SU(2) \times SU(3)$ gauge interactions, acting on quarks and leptons form the basis of the Standard Model (SM).

The SM contains the simplest possible Higgs sector, where a single Higgs doublet condenses in the vacuum, and gives masses to the gauge bosons and fermions. There is, however, no known principle for this simplicity.

Although very successful, however, the SM has yet been unable to provide an explanation for neutrino oscillations, the existence of dark matter, the baryon asymmetry of the Universe and other phenomena. Many New Physics (NP) models that give a solution to these problems predict additional particles and possibly and extended Higgs sector. Thus, it is essential to verify the structure of the Higgs sector and to see if it is indeed as in the SM or more complicated. The International Linear Collider (ILC) is capable of measuring gauge couplings, Yukawa couplings and Higgs self-couplings, giving us an overall picture of the Higgs sector. These couplings, might deviate from the SM in certain ways, depending on the structure of the Higgs sector and its underlying dynamics. Thus, measuring the Higgs couplings with high precision, might indicate us the direction towards NP [1].

TABLE I. – *Staging strategy of ILC. Both Luminosities are in* (fb^{-1})*, integrated over three years.*

E_{CM} (GeV)	250	500	1000
Running years	3	3	3
Canonical luminosity	250	500	1000
Luminosity-up	1150	1600	2500

2. – ILC the machine, and its strategy

One of the strong points of ILC is its ability to measure absolute Higgs couplings in a model-independent way. This is because at the ILC the center-of-mass energy can be gradually increased simply by extending the main linac. The ILC staging strategy is shown in table I: after a start at 250 GeV, there will be an increase of the CMS-energy to 500, and finally to 1000 GeV. In the three stages, an integrated luminosity of 250, 500 and 1000 fb^{-1} will be accumulated, respectively. With a luminosity upgrade, the accumulated luminosity will be 1150, 1600 and 2500 fb^{-1}, respectively [1].

3. – ILC characteristics and techniques

There are two main Higgs-production processes at the ILC: the Higgs-strahlung and the WW-fusion processes shown in fig. 1. The Higgs-strahlung process peaks at 250 GeV, while the WW-fusion process dominates at higher energies. At the ILC 80, 120 thousand Higgs events are produced at 250 GeV and 500 GeV, respectively. With a luminosity upgrade this amount is respectively quadrupled and tripled. For top-Yukawa coupling measurements the ttH-production process will be used, which is accessible above 500 GeV. At these higher energies focus will be not only on the measurement of the top-Yukawa coupling, but also on that of the Higgs self-couplings, and on the observation of low-statistics processes such as $H \to \mu\mu$.

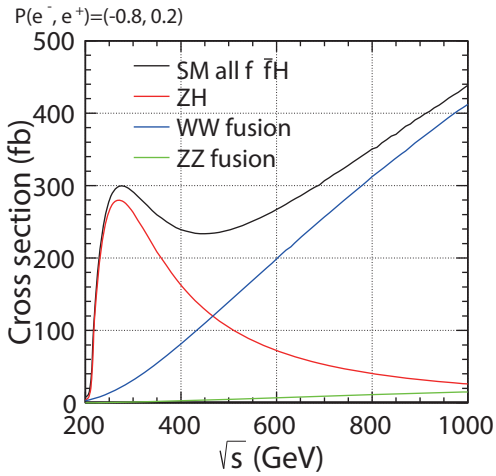

Fig. 1. – Higgs-production cross section.

The ILC is equipped with various tools to produce and capture Higgs efficiently and make model-independent measurements, which are also theoretically well understood. High polarization and high luminosity will enhance production rate and improve significance. Using a hermetic detector with high precision under a clean, low background environment enables high reconstruction efficiency of the signal event. Due to ILC's low background, bunch separation and collision rate conditions are extremely loose, enabling trigger-free operation, *i.e.* the acquisition of data without any bias. Finally, as for any lepton collider, elementary processes are theoretically well understood: at the ILC, kinematics can be solved and, with respect to the case of hadron colliders, as the Large Hadron Collider (LHC), there is less uncertainty arising from QCD ambiguity. Therefore deviations from SM predictions can be seen more clearly. Furthermore, in addition to the various observables obtained by kinematic information, ILC's ability to tune polarization and energy provides extra observables.

4. – ILC's expected sensitivity

4˙1. *ILC 250*. – At 250 GeV, the key to absolute Higgs coupling measurements is the Higgs recoil method using the Higgs-strahlung process. By reconstructing the Z boson from two leptons and solving kinematics, the ILC can capture the Higgs boson without looking at its decay product. Detection of invisible decays is, therefore, also possible. With the Higgs recoil method, the ILC can obtain absolute measurement of the g_{HZZ} coupling with a precision of 0.7%, and total cross section of ZH with 1.3% precision [1]. Since the ZH cross section appears in the denominator in the formula

$$Br(H \to XX) = \frac{\sigma_{ZH} Br(H \to XX)}{\sigma_{ZH}} \propto g^2_{HXX}, \tag{1}$$

used to extract Higgs couplings, a good precision on most of the g_{HXX} couplings can be expected. The most challening case is that of decays into b- and c-quarks or gluons. These decays can become backgrounds of each other, which make them hard to distinguish one from the other. ILC uses information such as number of lepton tracks and their momentum, decay length and mass to distinguish one from the other. The expected sensitivity for all model independent coupling measurements is summarized in table II.

4˙2. *ILC 500 and 1000*. – Above 500 GeV, the ttH- and the WW-fusion production processes can be used to extract the top-Yukawa coupling, the Higgs self-coupling, the Higgs total width, and to improve the measurement of other couplings.

4˙2.1. Higgs couplings and total width. A measurement of absolute Higgs couplings through WW-fusion is obtained by extracting the absolute normalization of g_{HWW} or the Higgs total width. This is done by measuring the cross section when the Higgs decays into bb and dividing that by the branching ratio $\mathrm{Br}(H \to bb)$, determined at 250 GeV:

$$\sigma_{\nu\nu H} Br(H \to bb) \propto g^2_{HWW} Br(H \to bb). \tag{2}$$

The HWW-coupling gives the Higgs total width:

$$\Gamma_{tot} = \frac{\Gamma_{HWW}}{Br(H \to WW^*)} \propto \frac{g^4_{HWW}}{\sigma_{\nu\nu H} Br(H \to WW^*)}\,. \tag{3}$$

TABLE II. – *Model-independent precisions* [1].

	ILC(250)	ILC(500)	ILC(1000)	ILC(LumUp)
$\sqrt{s}$ (GeV)	250	250+500	250+500+1000	250+500+1000
L (ab^{-1})	0.25	0.25+0.5	0.25+0.5+1	1.15+1.6+2.5
$\gamma\gamma$	18%	8.4%	4.0%	2.4%
gg	6.4%	2.3%	1.6%	0.9%
WW	4.8%	1.1%	1.1%	0.6%
ZZ	1.3%	1.0%	1.0%	0.5%
$t\bar{t}$	–	14%	3.1%	1.9%
$b\bar{b}$	5.3%	1.6%	1.3%	0.7%
$\tau^+\tau^-$	5.7%	2.3%	1.6%	0.9%
$c\bar{c}$	6.8%	2.8%	1.8%	1.0%
$\mu^+\mu^-$	91%	91%	16%	10%
$\Gamma_T(h)$	12%	4.9%	4.5%	2.3%
hhh	–	83%	21%	13%
BR(invis.)	$< 0.9\%$	$< 0.9\%$	$< 0.9\%$	$< 0.4\%$

Therefore by analyzing this process we can obtain absolute normalization of other couplings H decaying into X [2].

4˙2.2. Top-Yukawa coupling. The ttH-production process opens up above 500 GeV. Although the ttH cross section is small at 500 GeV and there are large combinatorial background events, due to QCD bound-state effects, the signal cross section is enhanced by a factor of two ($0.23 \to 0.45$ fb). This makes it possible to measure the top-Yukawa coupling. Increasing the center-mass energy will further enhance the cross section and with luminosity upgrade, an improvement of 14% to 2.0% is expected [1]. The pair-production threshold for top quarks can also be used for top-Yukawa coupling extraction [3], since the existence of Higgs exchange between top pairs will enhance the overall top pair-production cross section. A sensitivity of 4.2% for the Yukawa coupling can be achieved. This includes only experimental errors and does not include theoretical errors.

4˙2.3. Higgs self-coupling. In order to verify if the Higgs is indeed what condenses in the vacuum and gives masses to all the SM particles, we need to measure the Higgs self-coupling and measure the shape of the Higgs potential. The self-coupling is one of the most challenging to be measured at the ILC. In addition to its small cross section and large background, the existence of various irreducible diagrams dilutes the sensitivity to this coupling, as follows:

$$\frac{\delta\lambda}{\lambda} = 1.8\frac{\delta\sigma}{\sigma}\ (@500\,\text{GeV}), \qquad \frac{\delta\lambda}{\lambda} = 0.85\frac{\delta\sigma}{\sigma}\ (@1000\,\text{GeV}), \tag{4}$$

making it difficult to extract it. This dilution factor can be improved to 1.66 and 0.76 respectively using a new weighting method [1, 2]. High polarization helps improve the accuracy of cross section measurement. With the luminosity upgrade and the increase of energy to 1 TeV, measurement accuracy of 13% can be reached for $Z \to ll$ and qq, $HH \to 4b$ and $bbWW$ combined [4].

TABLE III. – *Model-dependent precisions* [1].

	ILC(250)	ILC(500)	ILC(1000)	ILC(LumUp)
$\sqrt{s}$ (GeV)	250	250+500	250+500+1000	250+500+1000
L (ab^{-1})	0.25	0.250+0.5	0.25+0.5+1	1.15+1.6+2.5
$\gamma\gamma$	17%	8.3%	3.8%	2.3%
gg	6.1%	2.0%	1.1%	0.7%
WW	4.7%	0.4%	0.3%	0.2%
ZZ	0.7%	0.5%	0.5%	0.3%
$t\bar{t}$	6.4%	2.5%	1.3%	0.9%
$b\bar{b}$	4.7%	1.0%	0.6%	0.4%
$\tau^+\tau^-$	5.2%	1.9%	1.3%	0.7%
$c\bar{c}$	6.8%	2.8%	1.8%	1.0%
$\mu^+\mu^-$	91%	91%	16%	10%
$\Gamma_T(h)$	9.0%	1.7%	1.1%	0.8%
hhh	–	83%	21%	13%
BR(invis.)	$< 0.9\%$	$< 0.9\%$	$< 0.9\%$	$< 0.4\%$

4˙3. *Full ILC.* – We summarize here the ILC expected precision. We can complete the Higgs-coupling measurements at 500 GeV and furthermore improve the sensitivity by combining results with increasing energy and luminosity. Improving the determination of absolute couplings at higher energies through the WW-fusion process is possible using the g_{Hbb} coupling obtained at 250 GeV through the Higgs-strahlung process. Therefore the measurement of the g_{Hbb} coupling at 250 GeV can set an upper-limit to the accuracy of Higgs couplings. An important advantage of increasing the ILC energy in terms of Higgs physics, other than improving accuracy, is the higher mass-reach for additional Higgs bosons expected in an extended Higgs sector and an higher sensitivity to the W_LW_L scattering to decide whether the Higgs sector is strongly interacting. The model-independent coupling sensitivity shown in table II can be achieved at full ILC run. With a model-dependent Higgs coupling parametrization proposed by the LHC Higgs Cross Section Working Group [5, 6], the sensitivity shown in table III can be achieved. Here it was assumed that 2nd-generation fermion Higgs couplings are related to those of the 3rd-generation couplings via $\kappa_c = \kappa_t$, $\kappa_\mu = \kappa_\tau$, and that the total width is the sum of all SM partial widths.

5. – Physics demands on International Large Detectors

This section is dedicated to address the technical difficulties of the previously mentioned analysis and introduce factors which drive detector technology, focusing on the International Large Detector (ILD). The most challenging are the measurements of Higgs self-coupling and of top-Yukawa coupling. These processes suffer from small signal cross section and large background events. Reducing combinatorial background events is crucial for improving sensitivity. Luminosity upgrade and polarization helps improving signal significance at the production level. To achieve high reconstruction efficiency and powerful discrimination power against background events, namely high quality lepton selection, flavour tagging and mass resolution are required. This implies excellent momentum resolution, impact parameter resolution and jet energy resolution for the de-

tector. In the following subsections the factors that determine detector designs for each sub-detector will be explained.

5˙1. *Vertex Detector*. – The vertex detector is responsible for high efficiency and high purity flavour tagging, which is particularly crucial for measuring Higgs self coupling(g_{hhh}) and g_{hcc} coupling. For example large tt backgrounds where $t\bar{t} \to bq\bar{q}\bar{b}q\bar{q}$ can be mistaken as a signal event $ZHH \to q\bar{q}b\bar{b}b\bar{b}$. Also $H \to c\bar{c}$ signal events can be buried in $H \to b\bar{b}$ large statistic events. The vertex detector is responsible for determining the impact parameter, which is essential for flavor tagging. Excellent impact parameter resolution can be achieved by low material, small spacial resolution, and by placing the detector close to the IP. This will, however, increase the amount of fake tracks caused by beam background events and degrade the efficiency and purity of flavor tagging. Therefor a vertex detector with both high impact parameter resolution and low pixel occupancy is needed:

$$\sigma_{r\phi} = 5\,\mu\mathrm{m} \oplus \frac{10}{p(\mathrm{GeV}\sin^{3/2}\theta)}\mu\mathrm{m}. \tag{5}$$

5˙2. *Time Projection Chamber*. – The time projection chamber (TPC) is the sub-detector responsible for momentum measurement. Momentum resolution is particularly driven by studies using the Higgs-strahlung process, where the recoiling Higgs is reconstructed from the associated Z boson decaying into a lepton pair. In order to achieve $\Delta\sigma_{ZH}/\sigma_H = 2.5\%$, $\Delta m_H = 30\,\mathrm{MeV}$ at 250 GeV ILC with $250\,\mathrm{fb}^{-1}$ integrated luminosity, which corresponds to the momentum resolution:

$$\sigma_{1/P_T} = 2 \times 10^{-5}\ [1/\mathrm{GeV}], \tag{6}$$

high-field magnets and high-precision/low-mass trackers are needed.

5˙3. *Calorimeter*. – Many physics processes at the ILC such as $Zh \to ZWW$ and $\nu\nu h \to \nu\nu WW$ require clean separation of hadronic decays of the W and Z boson. Effective separation better than $3\,\sigma$ in the mass peaks of the hadronic decays are required, which corresponds to precision:

$$\frac{\sigma_E}{E} = \frac{30\%}{\sqrt{E}} = 3 - 4\%\ (@100\,\mathrm{GeV}). \tag{7}$$

To achieve this unprecedented mass resolution, the ILD detector has adopted the particle flow approach by combining calorimetry and tracking. This technique of energy reconstruction makes use of the fact that many of the energy deposits in the calorimeter (on average about 65% of jet energies) are generated by charged tracks, which are very well measured by the tracker. Separation of such deposits from those generated in the calorimeter by neutral particles (photons and neutral hadrons) results in a much better energy measurement of jets. A calorimeter that can isolate and measure separately each individual particle contribution results in an optimal precision when the neutral energy measured in the calorimeter is combined with the charged energy measured in the tracker. The dominant limit comes from confusion within the calorimeter between the individual particle contributions. This motivates the requirement of high granularity of the electromagnetic and hadron calorimeters.

6. – State-of-the-art detector technology

There are several options with different technologies which are considered for the ILD.

6˙1. *Vertex Detector*. – Fine Pixel Charged Coupled Devices (FPCCDs) allow for particularly small pixels, $5 \times 5\,\mu\mathrm{m}^2$, which results in a sub-micron spatial resolution and excellent two-track separation capability [7]. The fine segmentation also mitigates occupancy issues and thus allows for integration over numerous bunch-crossings.

The DEPFET (Depleted P-channel Field Effect Transistor) concept integrates a p-MOS transistor in each pixel on the fully depleted, detector grade bulk silicon [8]. A DEPFET sensor generally is a 700×250 matrix of $50\times50\,\mu\mathrm{m}^2$ pixels. Electrons, produced in the bulk through ionizing radiation are collected in the internal gate and modulate the transistor current. Their low input capacitance ensures low noise operation.

CMOS Pixel Sensors (CPS). Matrices with 1152×576 pixels, with $18.4\,\mu\mathrm{m}$ pitch with a column parallel read-out architecture with amplification and correlated double sampling inside each pixel have been demonstrated [9]. A spatial resolution approaching $3\,\mu\mathrm{m}$ has been achieved with binary charge encoding.

6˙2. *Time Projection Chamber*. – The ILD concept is to achieve precision using a gas chamber capable of three dimensional track reconstruction. Tracks can be measured with a large number of three-dimensional (r, ϕ, z) space points. The point resolution, σ_{point}, and double-hit resolution, which are moderate when compared to silicon detectors, are compensated by continuous tracking. The TPC presents a minimum amount of material as required for the best calorimeter and PFA performance. A low material budget also minimizes the effects due to the 10^3 beamstrahlung photons per bunch-crossing that traverse the barrel region. Since low material is used, high gain electronics is essential for readout. Two options for the gas amplification systems are Micromegas [10] and Gas Electron Multipliers (GEM) [11]. At present either option would use pads of size $\approx 1 \times 6\,\mathrm{mm}^2$, resulting in about 10^6 pads per end-plate.

For a GEM readout two or three GEM foils are stacked together to achieve sufficient charge amplification. The transverse diffusion within the GEM stack itself is enough to spread the charge over several 1mm wide pads, which enables a good point reconstruction. Micromegas have enough amplification in a single structure, but the spatial extent of the signals is very small on the readout plane.

6˙3. *Electromagnetic Calorimeter(ECAL)*. – The principal role of the ECAL is to identify photons and measure their energy. For the particle flow jet reconstruction, but also for hadronic τ decays, the capability to separate photons from each other and from nearby hadrons is of primary importance. The large difference between electromagnetic radiation length and nuclear interaction length is thus one of the reasons for the choice of tungsten as absorber material, the other being its small *Molière* radius. Silicon pad diodes lead to the highest possible compactness (and effective *Molière* radius) and exhibit excellent stability of calibration. Scintillating strips with silicon photo-detector readout provide a similar effective segmentation and offer a less costly, but also somewhat less compact, option. Both technologies could be combined in order to reach a cost performance optimum.

6˙4. *Hadronic Calorimeter*. – The role of the Hadronic Calorimeter (HCAL) is to separate the deposits of charged and neutral hadrons and to precisely measure the energy

of the neutrals. Their contribution to the jet energy, around 10% on average, fluctuates widely from event to event, and the accuracy of the measurement is the dominant contribution to the particle flow resolution for jet energies up to about 100 GeV. For higher energies, the performance is dominated by confusion, and both topological pattern recognition and energy information are important for correct track cluster assignment. Stainless Steel with its moderate ratio of hadronic interaction length ($\lambda_I = 17\,\mathrm{cm}$) to electromagnetic radiation length ($X_0 = 1.8\,\mathrm{cm}$) allows a fine longitudinal sampling in terms of X_0 with a reasonable number of layers in a given total hadronic absorption length, thus keeping the detector volume and readout channel count small. This fine sampling is beneficial both for the measurement of the sizable electromagnetic energy part in hadronic showers as for the topological resolution of shower substructure, needed for particle separation and weighting. For the HCAL read-out, two options have been developed: one is based on scintillator tiles with silicon photo-sensors and analogue readout electronics, and the other is based on gaseous devices with one or two-bit, so-called semi-digital readout but finer transverse segmentation. The main gaseous technology pursued is glass resistive plate chambers (RPCs), but structures based on GEMs or Micromegas are being considered as alternatives.

REFERENCES

[1] Asner D. M., Barklow T., Calancha C., Fujii K., Graf N., Haber H. E., Ishikawa A., Kanemura S. *et al.*, arXiv, 1310 (0763) [hep-ph].
[2] Tian J. and Fujii K., arXiv, 1311 (6528) [hep-ph].
[3] Horiguchi T., Ishikawa A., Suehara T., Fujii K., Sumino Y., Kiyo Y. and Yamamoto H., arXiv, 1310 (0563) [hep-ex].
[4] Tian Junping *et al.*, LC-REP, 2013 (003).
[5] David A. *et al.*, *LHC HXSWG interim recommendations to explore the coupling structure of a Higgs-like particle 2012*, 1209 (0040).
[6] Dittmaier S., Mariotti C., Passarino G., Tanaka R., *et al.*, *Handbook of LHC Higgs Cross Sections:1. Inclusive Observables 2011*, 1101 (0593).
[7] Kato E. *et al.*, *Nuclear Science Symposium and Medical Imaging Conference (NSS/MIC), 2012 IEEE*, NSSMIC (2012) 6551171, 10 (1109).
[8] Hu-Guo C. *et al.*, *Nucl. Instrum. Methods A*, **623** (2010) 480.
[9] Lutz K., *Nucl. Instrum. Methods A*, **253** (1987) 365.
[10] Giomataris Y., Rebourgeard P., Robert J. P. and Charpak G., *Nucl. Instrum. Methods A*, **376** (1996) 29.
[11] Sauli F., *Nucl. Instrum. Methods A*, **386** (1997) 531.